Hindawi
International Journal of Corrosion
Volume 2018, Article ID 4728692, 10 pages
https://doi.org/10.1155/2018/4728692

Research Article

Study on the Electrochemical Performance of Sacrificial Anode Interfered by DC Stray Current

Qingmiao Ding, Tao Shen, Yanyu Cui, and Juan Xue

Airport College, Civil Aviation University of China, Tianjin, China

Correspondence should be addressed to Qingmiao Ding; qmding@cauc.edu.cn

Received 14 January 2018; Revised 27 May 2018; Accepted 27 June 2018; Published 1 August 2018

Academic Editor: Flavio Deflorian

The influence of sacrificial anode electrochemical properties interfered by direct stray current (DC) of 0 V, 1 V, 3 V, and 5 V, with different chloride ion concentration and temperature, was studied by open circuit potential (OCP), electrochemical impedance spectroscopy (EIS), and polarization curves. The specific performance was as follows: as the DC interference voltage increased from 0 V to 5 V, the degree of positive migration of the sacrificial anode open circuit potential increased. The effect of temperature in DC interference voltage environment on sacrificial anode corrosion was not great, but the low temperature of 10°C could slow down the sacrificial anode corrosion and maintain good work efficiency. With the increase of the ambient temperature, the degree of corrosion of the sacrificial anode was deepened. As the chloride ion concentration in DC interference voltage environment increased from 0% to 0.3%, the degree of positive migration of the sacrificial anode open circuit potential increased. The higher the chloride ion concentration was, the greater the impact on the performance of the sacrificial anode was.

1. Introduction

The cathodic protection system of airport apron pipe network generally adopts sacrificial anode cathodic protection [1], and the direct current stray current has a great influence on the potential and current of the pipeline, and it also inevitably has an adverse effect on the sacrificial anode performance [2]. DC stray current causes the fluctuations of pipeline potential and the required protective current to change greatly [3–8]. Therefore, it is necessary to make appropriate adjustments to the design of cathodic protection system with DC interference. In particular, the performance trend and mechanism of cathodic protection system using sacrificial anodes should be further clarified when it is disturbed by DC stray current [2]. The problem that the cathodic protection system interfered by DC stray current has become increasingly prominent. Airport apron pipeline network is the lifeblood of the airport. If the pipeline causes oil leakage due to corrosion, it is not only a serious threat to the safe operation of the pipeline, but also a hidden danger to the normal operation of the airport [2, 3]. Mustafa et al. [9] proposed that the microstructure and the state of the surface oxide film jointly determined the corrosion characteristics of the AZ63 magnesium alloy by researching the corrosion behavior of it in H_3PO_4/KOH buffer K_2SO_4 of pH=7.0. The pitting corrosion behavior of AZ63 magnesium alloy in NaCl solution was studied by Chen Lin et al. [10]. It was found that, in high concentration NaCl solution, the pitting pit was difficult to film. And the uniform corrosion characteristic was present to the magnesium alloy while the corrosion rate of the magnesium alloy increased. Liu Xianguo et al. [11] used the admixture method which was added to the alloy between Mg and Sr to obtain the best process parameters of the Mg-Sr alloy. Chen Kun et al. [12] based on Al-Zn-In alloy added different content ratios of Mg and Si. It was found that 0.09% Si and 1.0% Mg were the optimal element additions for optimum anode electrochemical performance. Zhang Qiumei et al. [13] discussed the effects of Mn contents on the electrochemical properties of the Mg-Mn anodes and Ca, Sr contents on the microstructure and the electrochemical performance of the Mg-(Mn)-X anodes and the effects of melting and casting process and extrusion process on the electrochemical performance of the magnesium and the working principle of the low potential resistance magnesium

Table 1: Composition of soil simulated solution.

Composition	Content
Distilled water(ml)	1000
Na_2CO_3(g)	0.1599
NaCl(g)	0.5124
Na_2SO_4(g)	0.1712
$NaHCO_3$(g)	0.0864

anode. In previous studies, most of them researched how to improve the electrochemical performance of magnesium alloys and their limitations as anode materials. The effect of DC stray current on the sacrificial anode performance has not been studied. Therefore, it is very necessary to study the influence of DC stray current on the cathodic protection system.

2. Experimental Program

2.1. Soil Simulated Solution. The soil simulated solution was get from the soil of an apron. Its composition was as shown in Table 1.

2.2. Experimental Materials. The experiment used three-electrode system with reference electrode (saturated calomel electrode), auxiliary electrode (platinum electrode), and working electrode. The working electrode materials were magnesium alloy rods with diameter of 10 mm. The magnesium alloy sacrificial anode rods were welded with the wire and the welded anode was put into the electrician tubes for the preparation of the electrode. Use epoxy resin and curing agent mixture with the ratio of 3:1 to pour the electrode and reserve the working face. We could get the working electrodes after the overnight standing. The magnesium alloy sacrificial anode ingredients used in this experiment were shown in Table 2.

2.3. Test Method and Content

2.3.1. The Open Circuit Potential. The magnesium alloy sacrificial anode was immersed in the solution for three hours before the experiment. Then the open circuit potential could be measured. The sacrificial anode was kept under full immersion for 15 minutes and then the open circuit potential was measured in each period.

2.3.2. Polarization Curves. According to the test results of open circuit potential, it was determined that the range of polarization curve was -0.8 V to -0.3 V, and the scanning rate was 0.1667 mV/s. The experimental instrument was an electrochemical workstation.

2.3.3. Electrochemical Impedance Spectroscopy (EIS). After the open potential of the sacrificial anode was stable, it was measured under the condition of relative open circuit potential. The frequency range of the test was 100 kHz to 0.1 Hz, the amplification of sinusoidal AC signal was 3 mV, and 72 points were tested in total. The data analysis software was ZSimpWin3.21.

3. Results and Discussion

It was found that the apron pipelines used magnesium alloy sacrificial anode through the investigation. At the apron pipelines operating environment, in addition to the interference of DC stray current in sacrificial anode, chloride ion and temperature also affected the electrochemical performance of sacrificial anode. So we focused on how DC stray current and chloride ion concentration and temperature influenced sacrificial anode electrochemical properties. And we did parallel experiments to ensure the accuracy of the experiment and the reproducibility of the data.

3.1. The Open Circuit Potential of Sacrificial Anode. The E-t curves of magnesium sacrificial anodes under different influence factors were shown in Figure 1.

3.1.1. The Effect of DC Stray Current. As shown in Figure 1(a), at the beginning of the experiment, the open circuit potential of sacrificial anode was in the most negative state, so the corrosion tendency was the highest. The open circuit potential of the sacrificial anode was always shifted in a more positive direction during the experiment, and it indicated that the activity in the sacrificial anode surface was decreasing as the experiment goes on. In four different DC disturbances (0 V, 1 V, 3 V, and 5 V), the positive migration of the open circuit potential with 0 V interference voltage was smaller than other disturbances on the second day. In the last six days, the trend of potential changes shifted slowly and positively. But the amount of offset was different, and the general trend was that the open circuit potential's positive migration with 5 V interference voltage was the maximum while that with 0 V interference voltage was the minimum. It showed that the existence of DC stray current reduced the corrosion dissolution tendency of the sacrificial anode. And within a certain range, the larger the DC stray current interference voltage was, the greater the impact on it was.

3.1.2. The Effect of Ambient Temperature. As shown in Figure 1(b), at the beginning of the experiment, the open circuit potential was in the most negative state, and the corrosion tendency was the highest. In the first two days which was the early experiment, the positive migration of the open circuit potential at 10°C was smaller than that at room temperature environment and 30°C. In the last six days, the trend of potential changes shifted slowly and positively. Although the amount of offset was different, the degree of the open circuit potential migration was not very different. The general trend was that the open circuit potential's positive migration at 30°C was the maximum while that at 10°C was the minimum. It showed that the change of ambient temperature had little effect on the degree of sacrificial anode corrosion with the influence of DC stray current, but there was also a certain rule. The degree of sacrificial anode corrosion increased with the rising of the temperature.

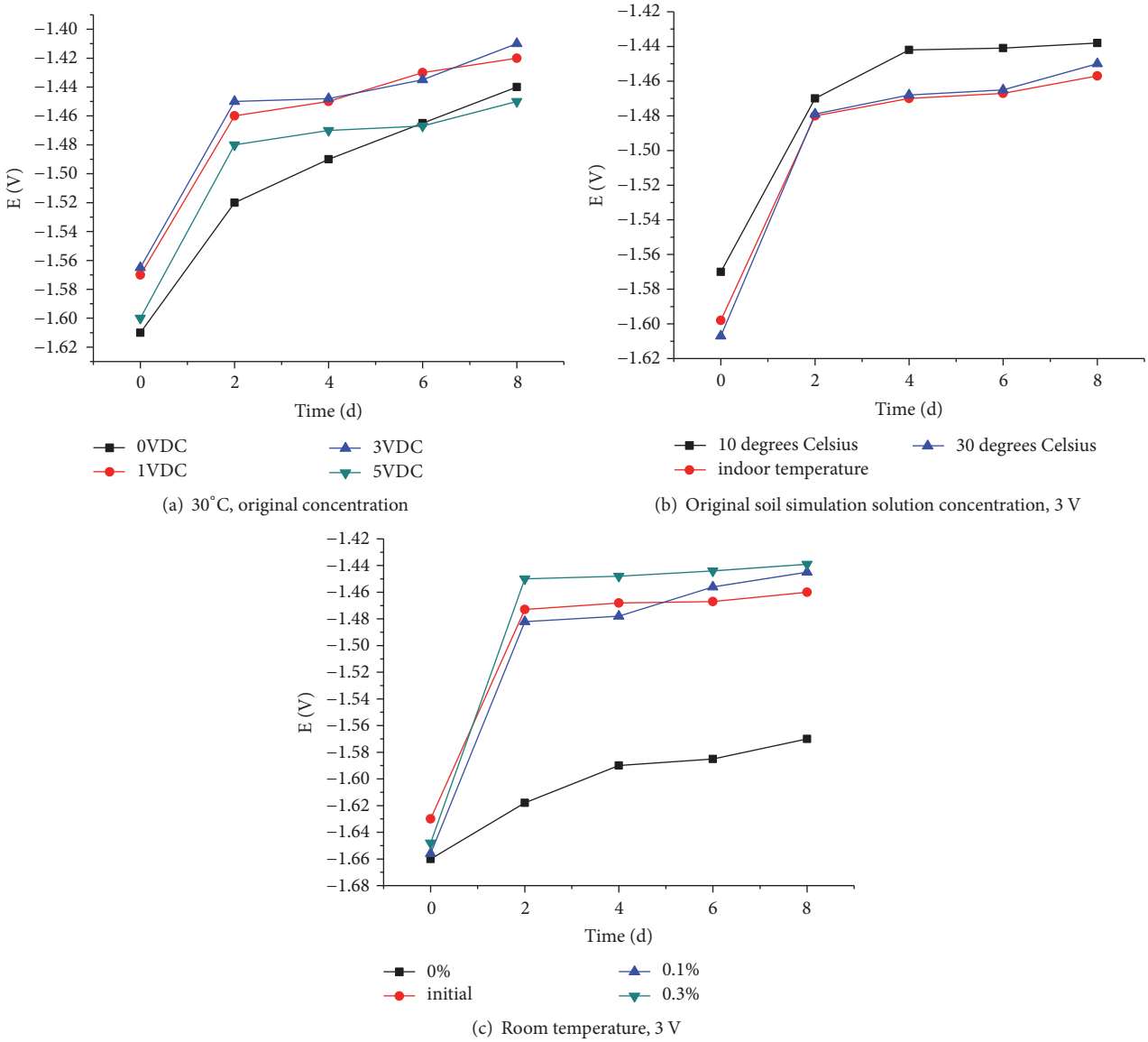

(a) 30°C, original concentration

(b) Original soil simulation solution concentration, 3 V

(c) Room temperature, 3 V

Figure 1: E-t curves of magnesium sacrificial anode with different influencing factors.

Table 2: Magnesium alloy sacrificial anode ingredients.

Al(%)	Zn(%)	Mn(%)	Fe(%)	Ni(%)	Cu(%)	Si(%)	Mg(%)
6.5	3.5	0.6	0.005	0.003	0.02	0.1	89.272

3.1.3. The Effect of Chloride Ion Concentration. As shown in Figure 1(b), at the beginning of the experiment, the open circuit potential of sacrificial anode was in the most negative state, and the corrosion tendency was the highest. The open circuit potential of the sacrificial anode was always shifted in a more positive direction during the experiment, and it indicated that the sacrificial anode surface activity was decreasing as experiment goes on. In four different chloride ion concentrations (0%, original soil simulation solution concentration, 0.1%, and 0.3%), the open circuit potential's positive migration of the chloride ion concentration of 0% was smaller than other situations on the second day. The degree of the positive migration in the environment with 0.3% chloride ion was the biggest. In the last six days, the trend of potential changes shifted slowly and positively. Although the amount of offset was different, the degree of the open circuit potential migration was not very different. The general trend was that the open circuit potential's positive migration with 3% chloride ion was the maximum while that with 0% chloride ion was the minimum. The degree of the migrant with 0.1% chloride ion and original soil simulation solution concentration was between them. It indicated that the change of chloride ion concentration had great effect on the degree of sacrificial anode corrosion under the influence

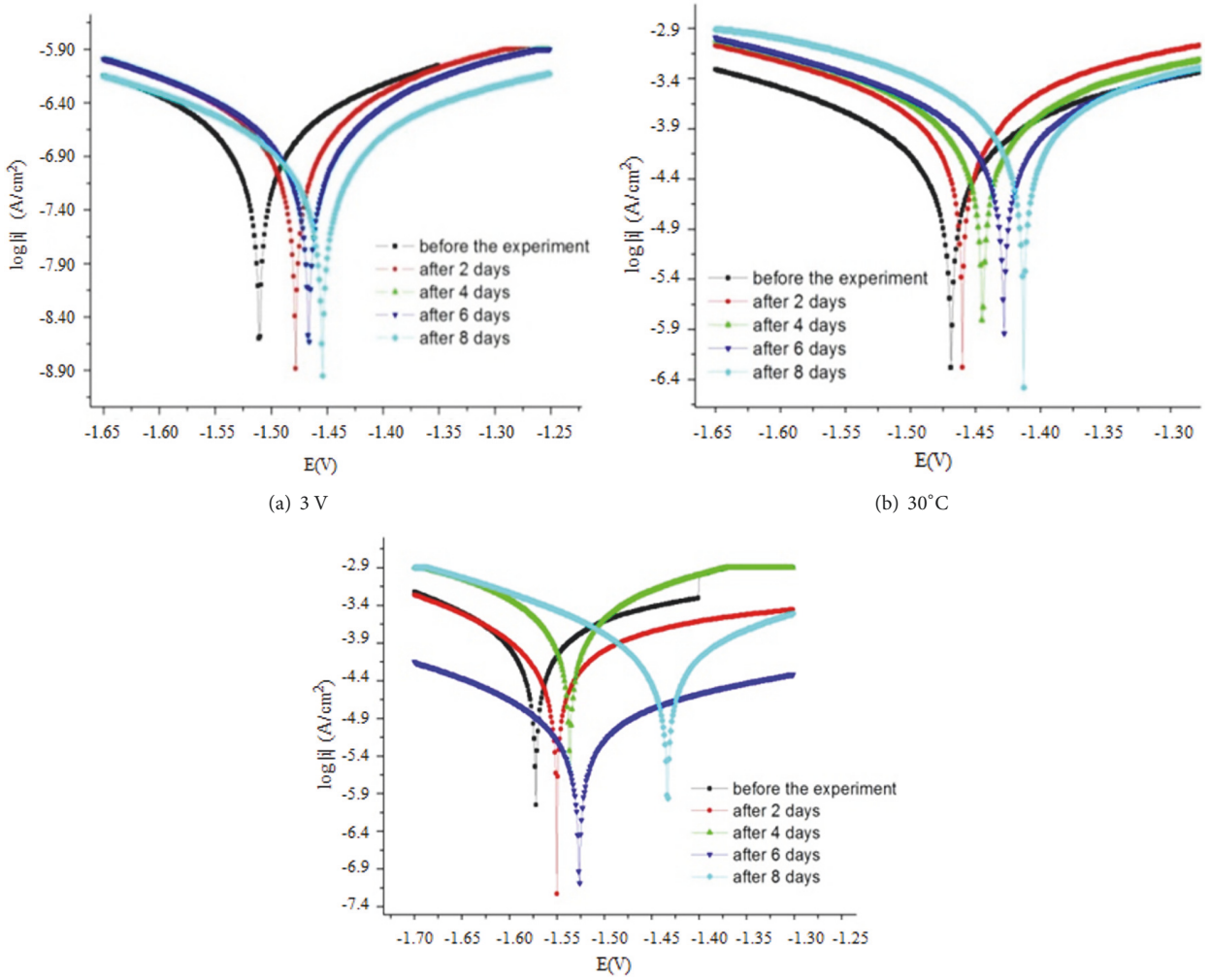

(a) 3 V

(b) 30°C

(c) The chloride ion concentration of 0.3%

Figure 2: Polarization curves of magnesium sacrificial anode with different influence factors.

of DC stray current. With the increase of the concentration of chloride ion, the corrosion degree of the sacrificial anode increased obviously. And the chloride ion was a major indicator of the electrochemical performance of the sacrificial anode.

3.2. Polarization Curves. The polarization curves under different influence factors were shown in Figure 2.

3.2.1. The Effect of DC Stray Current. The corrosion electrochemical parameters of the sacrificial anode under different DC voltages were shown in Table 3.

As shown in Table 3, the ratio of anodic slope and cathode slope with DC stray current was less than that with no stray current in the same period, and it indicated that the rate of corrosion was accelerated under stray current interference. The ratio of anodic slope and cathode slope in the case of 5 V was the minimum while that in the case of 3 V was the maximum. The ratio of anodic slope and cathode slope in the case of 0 V and 1 V was between them. It showed that the effect of 5 V was the greatest and the effect of 3 V was the smallest.

By comparing the polarization resistance and corrosion current density of sacrificial anode with different stray current interference, it was found that the polarization resistance of sacrificial anode was the largest and the corresponding polarization current was the smallest under the condition with 0 V interference. The sacrificial anode polarization resistance with 3 V interference was larger, and the corrosion current density was smaller. The sacrificial anode polarization resistance with 5 V interference was the smallest, and the corrosion current density was the largest, followed by that with 1 V interference. It showed that the influence of DC voltage on the sacrificial anode was not good, because it increased the corrosion rate of sacrificial anode. The sacrificial anode corrosion under DC stray current of 3 V mitigated. The passivation layer might be easier to form in the corrosion products attached to the sacrifice anode corrosion surface in this condition. It played a role to protect the metal surface. So

Table 3: The corrosion electrochemical parameters of the sacrificed anode interfered with different DC voltage.

Experiment days (d)	DC voltage (V)	Cathodic slope	Anodic slope	Polarization resistance ($\Omega*cm^2$)	Corrosion current density ($\mu A/mm^2$)
0	0	-6.35	5.772	5.161	0.83
	1	-5.131	4.834	2.184	2.31
	3	-5.191	4.386	2.608	1.74
	5	-5.392	4.653	1.781	2.43
2	0	-4.738	5.027	5.741	0.74
	1	-5.813	4.396	3.670	1.63
	3	-4.729.	5.495	5.363	1.59
	5	-5.037	4.701	2.049	2.11
4	0	-5.092	5.168	7.206	0.43
	1	-4.641	5.0821	4.693	0.98
	3	-4.447	5.372	6.452	0.66
	5	-5.623	5.372	2.164	2.08
6	0	-4.438	5.172	9.561	0.43
	1	-4.713	5.626	5.775	0.76
	3	-4.732	4.916	7.354	0.52
	5	-5.151	5.517	2.405	1.87
8	0	-5.405	5.88	12.063	1.55
	1	-4.724	5.118	6.379	0.71
	3	-4.251	4.976	8.018	0.49
	5	-4.233	4.777	3.681	0.22

the corrosion current density decreased and the corrosion of metal slowed down.

3.2.2. The Effect of Ambient Temperature. The corrosion electrochemical parameters of the sacrificial anode at different ambient temperatures were shown in Table 4.

As shown in Table 4, we could know that the ratio of cathodic slope to anodic slope increased with the rising of ambient temperature at the same time. It indicated that the rise of ambient temperature accelerated the corrosion of sacrificial anode. Through the comparative study on the sacrificial anode polarization resistance and corrosion current density at different temperature, we could find that the anode polarization resistance was the maximum and the corresponding corrosion current density was the minimum in 10°C, while the situation was opposite in 30°C. It indicated that the degree of the sacrificial anode corrosion increased with the rising of the temperature.

3.2.3. The Effect of the Concentration of Chloride Ion. The corrosion electrochemical parameters of the sacrificial anode at different chloride ion concentration of chloride ion were shown in Table 5.

As shown in Table 5, at the same time, the ratio of cathodic slope to anodic slope increased with the increase of the chloride ion concentration. It indicated that the higher the chloride ion concentration was, the faster the sacrificial anode corrosion rate was. Through the comparative study on the polarization resistance and corrosion current density of the sacrificial anode with different chloride ion concentration, it was found that the polarization resistance was the maximum and the corrosion current density was the minimum without chloride ion, while the polarization resistance was the minimum and the corrosion current density was the maximum in the concentration of 0.3% chloride ion concentration. It indicated that the corrosion rate of the sacrificial anode increased with the increasing of chloride ion concentration and the corrosion degree was obviously aggravated.

3.3. Electrochemical Impedance Spectroscopy. The electrochemical impedance spectroscopy (EIS) under different influence factors was shown in Figure 3.

In this experiment, the electrochemical impedance spectrum under different conditions was replaced by equivalent circuit (CR (CR)) through ZSimpWin software, and the error was controlled within the allowable range. The different elements represented different physical meanings: R0 represented the resistance of the solution. C1 represented the electric double layer capacitor of the metal oxide film and the solution. C2 represented the capacitance that is due to the ion through surface oxide film. R1 represented the oxidation resistance. When the experiment started, the oxide film on the surface of the sacrificial anode was destroyed, and the exposing metal reacted with oxygen. The corrosion products began to accumulate on the surface of the sacrificial anode. The physical meaning of the element representation changed:

Table 4: The corrosion electrochemical parameters of the anode at different ambient temperature.

Experiment days (d)	Ambient temperature (V)	Cathodic slope	Anodic slope	Polarization resistance ($\Omega*cm^2$)	Corrosion current density ($\mu A/mm^2$)
0	10°C	-5.234	4.802	2.208	1.85
	room-temperature	-5.131	4.834	2.184	2.19
	30°C	-4.954	4.153	2.177	2.31
2	10°C	-4.738	5.027	3.688	1.47
	room-temperature	-5.072	5.106	3.670	1.62
	30°C	-4.931	5.274	2.781	1.63
4	10°C	-5.215	5.723	4.693	0.92
	room-temperature	-4.641	5.0821	4.599	0.98
	30°C	-4.624	5.023	3.593	1.11
6	10°C	-5.378	5.615	5.857	0.76
	room-temperature	-4.713	5.026	5.775	0.83
	30°C	-4.858	4.964	3.876	1.02
8	10°C	-5.495	6.362	6.439	0.71
	room-temperature	-4.724	5.118	6.379	0.71
	30°C	-4.582	4.954	4.068	0.75

Table 5: The corrosion electrochemical parameters of the anode under different chloride ion concentration conditions.

Experiment days (d)	Chloride ion concentration	Cathodic slope	Anodic slope	Polarization resistance ($\Omega*cm^2$)	Corrosion current density ($\mu A/mm^2$)
0	0%	-5.234	4.497	5.058	0.87
	origin	-5.131	4.834	2.184	2.31
	0.1%	-5.219	5.031	1.387	3.06
	0.3%	-6.221	5.213	0.805	4.79
2	0%	-4.565	4.716	5.581	0.72
	origin	-4.738	5.027	3.670	1.61
	0.1%	-5.343	5.134	2.871	1.63
	0.3%	-6.178	5.562	2.575	1.79
4	0%	-4.432	4.911	6.570	0.57
	origin	-4.641	4.821	4.693	0.97
	0.1%	-5.019	5.076	4.587	0.98
	0.3%	-6.038	5.713	2.930	1.14
6	0%	-4.572	4.702	7.123	0.53
	origin	-4.713	4.926	6.023	0.63
	0.1%	-4.934	5.123	5.775	0.76
	0.3%	-5.997	5.803	4.853	0.98
8	0%	-4.544	4.932	8.157	0.48
	origin	-4.724	5.118	7.718	0.54
	0.1%	-4.872	5.021	7.103	0.71
	0.3%	-5.846	5.916	6.379	0.82

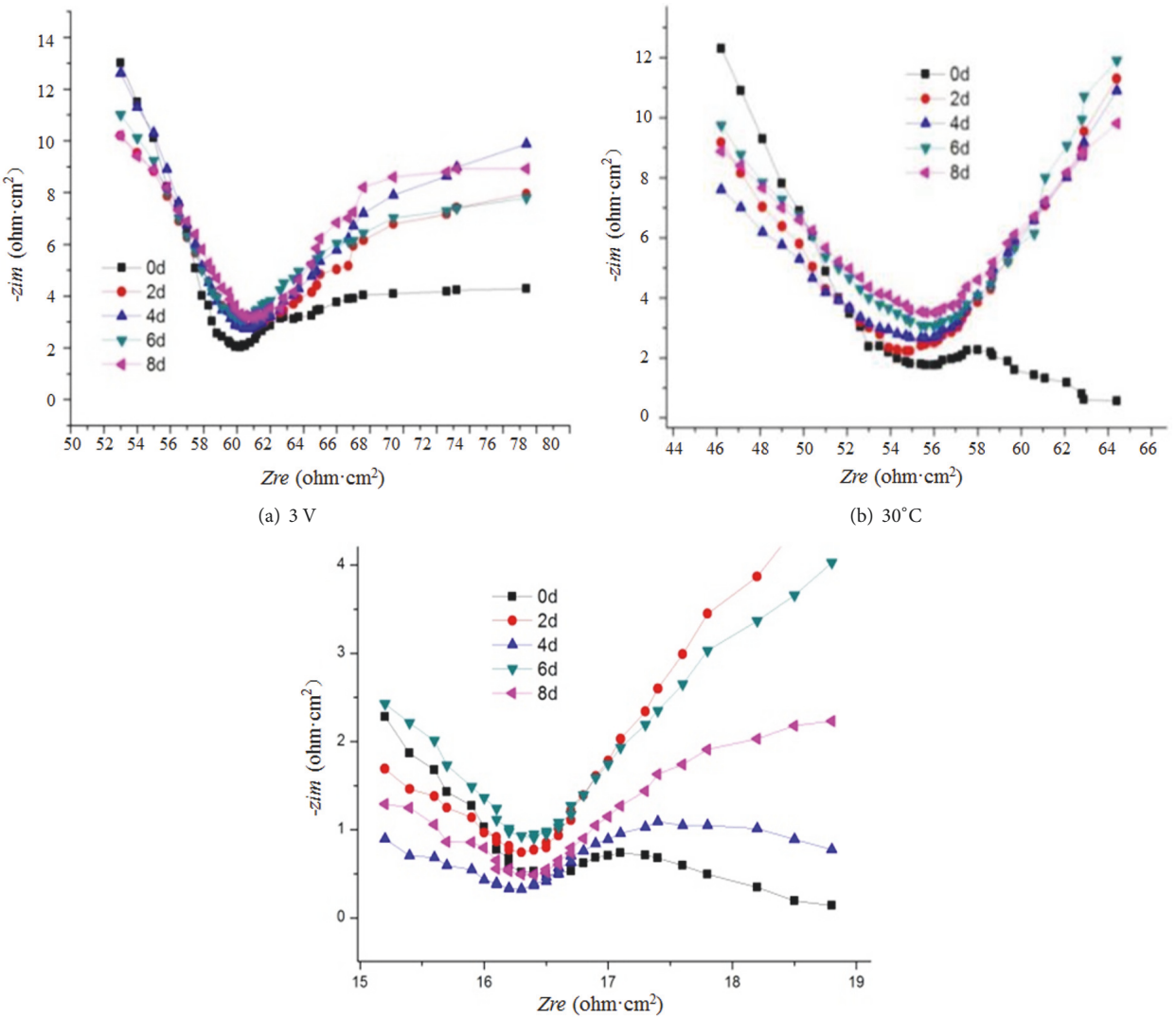

(a) 3 V

(b) 30°C

(c) The chloride ion concentration of 0.3%

Figure 3: Electrochemical impedance spectra of the sacrificial anode with different influence factors.

R0 still represented the resistance of the solution and C1 still represented the electric double layer capacitor of the oxide film and the solution, and C2 no longer expressed the capacitance that is due to the ion through surface oxide film, but on behalf of the capacitance that is due to the ion through corrosion scale. Rc represented the corrosion product film resistance. The circuit diagram was shown in Figure 4.

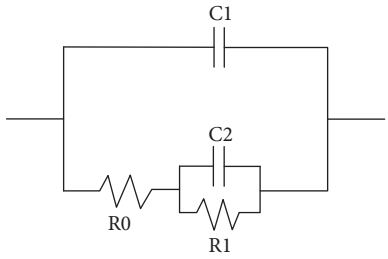

Figure 4: Equivalent circuit of the sacrificial anode process.

3.3.1. The Effect of DC Stray Current. The equivalent circuit diagram could be synthesized by ZSimpWin software, and the required resistance could be further calculated. The fitting results were shown in Table 6.

From Table 6, we could see that the resistance of the solution with no DC interference was larger than that with DC interference. It indicated that the sacrificial anode corrosion rate was faster with DC interference. Under the condition of interference, the solution resistance of 5 V was the smallest while the solution resistance of 3 V was the largest. It indicated that the corrosion rate was the fastest under the condition of 5V, and the corrosion rate was relatively slow under the condition of 3 V. During the experiment, the resistance of the oxide film increased with the passing of the experimental period, and it indicated that the corrosion products adhered to the sacrificial anode surface increased as

Table 6: The resistance parameters of the fitted equivalent circuit.

Interference voltage (V)	Experiment days (d)	Solution Resistance ($\Omega*cm^2$)	Oxide film Resistance ($\Omega*cm^2$)
0	0	0.473	0.111
	2	0.538	0.367
	4	0.638	0.390
	6	0.733	0.477
	8	0.805	0.620
1	0	0.462	0.128
	2	0.505	0.351
	4	0.627	0.486
	6	0.690	0.497
	8	0.758	0.686
3	0	0.461	0.120
	2	0.520	0.362
	4	0.665	0.394
	6	0.712	0.482
	8	0.768	0.601
5	0	0.482	0.135
	2	0.485	0.375
	4	0.598	0.494
	6	0.572	0.620
	8	0.449	0.725

experiment goes on. The oxidation resistance change with DC interference was bigger than that with no DC interference, indicating that the degree of the sacrificial anode corrosion with DC stray current interference was larger. DC stray current promoted the corrosion products on the surface of sacrificial anode and reduced the resistance of anode surface corrosion reaction and then accelerated the sacrificial anode corrosion.

3.3.2. The Effect of Ambient Temperature. The resistance parameters of the fitting equivalent circuit were shown in Table 7.

As shown in Table 7, the resistance of solution at 10°C was larger than that at the room temperature or 30°C, indicating that the corrosion rate of sacrificial anode was slower at 10°C. As the temperature of the environment rose, the corrosion rate of the sacrificial anode increased and the effect on the performance of the sacrificial anode was greater. During the experiment, the resistance of the oxide film increased with the passing of the experiment period, indicating that the corrosion products adhered to the sacrificial anode surface increased with the increasing of time. The change of resistance of sacrificial anodic oxide film was greater with the increasing of temperature, indicating that the increasing of ambient temperature promoted the production of corrosion products at the sacrificial anode surface and reduced the resistance of sacrificial anode surface corrosion reaction and then accelerated the sacrificial anode corrosion. However, the change of temperature had little effect on the change range of the oxide film resistance, indicating that the temperature had little effect on the performance of the sacrificial anode.

3.3.3. The Effect of Chloride Ion Concentration. The resistance parameters of the fitting equivalent circuit were shown in Table 8.

It could be seen from Table 8 that the solution resistance at 0% chloride ion concentration was larger than that in the presence of chloride ion at the same time, indicating that the sacrificial anode corrosion rate was very slow at this condition. In the presence of chloride ion, the solution resistance decreased with the increasing of chloride ion concentration, indicating that the increasing of chloride ion concentration accelerated the sacrificial anode corrosion. And the resistance of the oxide film at 0% chloride ion concentration in the same period was much higher than that in the presence of chloride ion, indicating that the sacrificial anode corrosion reaction was very slight at this time. The resistance varied greatly with the development of time in the presence of chloride ion, which indicated that the presence of chloride ion accelerated the generation of corrosion products at the sacrificial anode surface and reduced the resistance of sacrificial anode surface corrosion reaction and then accelerated the sacrificial anode corrosion. The resistance change at 0.3% chloride ion concentration was very irregular, and it could be judged that the sacrificial anode corrosion was very serious at this time. The corrosion products continuously formed and fell off and then formed and fell off again.

Table 7: The resistance parameters of the fitted equivalent circuit.

Ambient temperature (°C)	Experiment days (d)	Solution Resistance ($\Omega*cm^2$)	Oxide film Resistance ($\Omega*cm^2$)
10°C	0	0.351	0.143
	2	0.423	0.172
	4	0.432	0.233
	6	0.482	0.245
	8	0.513	0.327
room-temperature	0	0.347	0.144
	2	0.391	0.195
	4	0.419	0.233
	6	0.473	0.263
	8	0.498	0.363
30°C	0	0.346	0.143
	2	0.372	0.209
	4	0.413	0.244
	6	0.469	0.278
	8	0.497	0.382

Table 8: The resistance parameters of the fitted equivalent circuit.

Chloride ion concentration	Experiment days (d)	Solution Resistance ($\Omega*cm^2$)	Oxide film Resistance ($\Omega*cm^2$)
0%	0	0.723	0.292
	2	0.739	0.476
	4	0.880	0.487
	6	0.915	0.535
	8	1.156	0.574
Origin	0	0.462	0.135
	2	0.505	0.362
	4	0.627	0.394
	6	0.690	0.482
	8	0.758	0.554
0.1%	0	0.269	0.030
	2	0.299	0.089
	4	0.320	0.116
	6	0.339	0.279
	8	0.384	0.122
0.3%	0	0.106	0.012
	2	0.130	0.226
	4	0.134	0.060
	6	0.144	0.095
	8	0.153	0.038

4. Conclusion

(1)Under the same ambient temperature and the same chloride ion concentration, as the DC stray current interference increased from 0 V to 5 V, the degree of positive migration of the sacrificial anode open circuit potential increased and the existence of DC stray current affected the efficiency of sacrificial anode. In the same period, the corrosion current density of the DC stray current at 3 V was relatively small, which slowed down the corrosion of the sacrificial anode.

(2)The effect of temperature in the environment with DC interference voltage on sacrificial anode corrosion was

not great, but the low temperature of 10°C could slow down the sacrificial anode corrosion and maintain good work efficiency. With the increase of the ambient temperature, the degree of corrosion of the sacrificial anode was deepened.

(3) As the chloride ion concentration in the environment with DC interference voltage increased from 0% to 0.3%, the degree of positive migration of the sacrificial anode open circuit potential increased. The higher the chloride ion concentration was, the greater the impact on the performance of the sacrificial anode was.

Data Availability

The data used to support the findings of this study are available from the corresponding author upon request.

Conflicts of Interest

The authors declare that there are no conflicts of interest regarding the publication of this article.

Acknowledgments

The research work was supported by the Central College Foundation of CAUC (Grant no. 3122017038).

References

[1] Z. Zhou, J. Ling, B. Liang, and C. Huang, "Analysis on additional stress for apron oil pipe under external loads," *Tongji Daxue Xuebao/Journal of Tongji University*, vol. 41, no. 8, pp. 1219–1262, 2013.

[2] M. Narozny, K. Zakowski, and K. Darowicki, "Method of sacrificial anode dual transistor-driving in stray current field," *Corrosion Science*, vol. 98, pp. 605–609, 2015.

[3] S. Qian and Y. F. Cheng, "Accelerated corrosion of pipeline steel and reduced cathodic protection effectiveness under direct current interference," *Construction and Building Materials*, vol. 148, pp. 675–685, 2017.

[4] A. Aghajani, M. Urgen, and L. Bertolini, "Effects of DC stray current on concrete permeability," *Journal of Materials in Civil Engineering*, vol. 28, no. 4, 2016.

[5] C. Yang, G. Cui, Z. Li, Y. Zhao, and C. Zhang, "Study the influence of DC stray current on the corrosion of X65 steel using electrochemical method," *International Journal of Electrochemical Science*, vol. 10, no. 12, pp. 10223–10231, 2015.

[6] G. Lucca, "Estimating stray current interference from DC traction lines on buried pipelines by means of a Monte Carlo algorithm," *Electrical Engineering*, vol. 97, no. 4, pp. 277–286, 2015.

[7] C. Wen, J. Li, S. Wang, and Y. Yang, "Experimental study on stray current corrosion of coated pipeline steel," *Journal of Natural Gas Science and Engineering*, vol. 27, pp. 1555–1561, 2015.

[8] S.-Y. Xu and W. Li, "Research on stray current corrosion evaluation of buried metallic pipeline in an urban rail transit system," *International Journal of Electrochemical Science*, vol. 10, no. 7, pp. 5950–5960, 2015.

[9] M. Anik and I. M. Guneşdoğdu, "Corrosion characteristics of Alloy AZ63 in buffered neutral solutions," *Materials and Corrosion*, vol. 31, no. 6, pp. 3100–3105, 2010.

[10] C. Lin, C. Jing, and S. Yang, "Study on pitting and corrosion inhibition of AZ63 magnesium alloy in sodium chloride solution," *Surface Technology*, vol. 42, no. 05, pp. 24–28, 2013.

[11] X.-G. Liu, X.-D. Peng, W.-D. Xie, and Q.-Y. Wei, "Preparation technologies and applications of strontium-magnesium master alloys," *Materials Science Forum*, vol. 488-489, pp. 31–34, 2005.

[12] C. Kun, C. Qin, G. Chaowen et al., "Correlation between microstructure and properties of Aluminum alloy sacrificial anodes containing Mg in the seawater environment," *Journal of Guangxi Academy of Sciences*, vol. 33, no. 03, pp. 195–199, 2017.

[13] Z. Qiumei, H. Juncai, and L. Guojun, "Current status of Magnesium-based sacrificial anodes," *Foundry Technology*, vol. 31, no. 7, pp. 938–941, 2010.